WPPFC-CPR(17) 16939

M Kelemen et al.

Micro-NRA with microbeam on samples exposed in ASDEX Upgrade

Preprint of Paper to be submitted for publication in Proceeding of 16th International Conference on Plasma-Facing Materials and Components for Fusion Applications

This work has been carried out within the framework of the EUROfusion Consortium and has received funding from the Euratom research and training programme 2014-2018 under grant agreement No 633053. The views and opinions expressed herein do not necessarily reflect those of the European Commission.

Study of lateral distribution of impurities on samples exposed in ASDEX Upgrade by microbeam

Mitja Kelemen[1,2*], Anže Založnik[1], Primož Vavpetič[1], Primož Pelicon[1], Antti Hakola[3], Gerd Meisl[4], Martin Oberkofler[4], Karl Krieger[4], Sebastijan Brezinsek[5] the ASDEX Upgrade Team[4], EUROfusion MST1 Team[a] and Sabina Markelj[1]

[1] Jožef Stefan Institute, Jamova 39, SI-1000 Ljubljana, Slovenia

[2]Jožef Stefan International Postgraduate School, Jamova cesta 39, 1000 Ljubljana, Slovenia

[3] VTT Technical Research Centre of Finland Ltd, P O Box 1000, FI-02044, VTT, Finland

[4] Max-Planck-Institut für Plasmaphysik, Boltzmannst. 2, D-85748 Garching, Germany

[5] Forschungszentrum Jülich GmbH, Institut für Energie- und Klimaforschung Plasmaphysik, Partner of the Trilateral Euregio Cluster, 52425 Jülich, Germany

[a] See the author list of "Overview of progress in European Medium Sized Tokamaks towards an integrated plasma-edge/wall solution" by H. Meyer et al., to be published in Nuclear Fusion Special issue: Overview and Summary Reports from the 26th Fusion Energy Conference (Kyoto, Japan, 17-22 October 2016)

***Corresponding author: Mitja Kelemen**

E-mail address: mitja.kelemen@ijs.si

Abstract

In this paper we present the use of focused ion beams to study the distribution of deuterium (D), boron (B) and nitrogen (N) on tungsten (W) samples exposed in the divertor region of ASDEX Upgrade during ^{15}N-seeded L-mode discharges in deuterium and during non-seeded H-mode discharges in helium. After the ^{15}N experiment three types of samples of various surface roughness were analysed: 100 nm thick W coatings on milled or polished graphite substrates and bulk W samples, ranging from roughest (milled) to smoothest (bulk W). We found that D, N and B are distributed quite homogeneously over the sample on the micrometer scale with some small variation inside of the analysed area. The amounts show strong variations in the poloidal direction, with peaks values at or around the strike point. The variations of the retained impurities (D, B, N) over the analyzed spots are more or less correlated. The amounts of retained (D, B, N) are strongly corelated to the surface roughness of the samples, being highest in the rough samples. We observed some surface scratches due to arc strikes on microscale 2D maps of W on the studied samples which cannot be correlated with impurity distributions. Samples originating from the He campaign in AUG show inhomogeneous distribution of impurities with micro-scale structure which is most pronounced on pre-damaged W sample, where rough fuzz-like structure surface is create during exposure in GLADIS machine.

Keywords: Focused ion beams, Deuterium, ^{3}He, Nuclear Reaction Analysis, PIXE

Introduction

One of the key research areas in the field of plasma-surface interactions is erosion and migration of impurity species. Migration influences erosion and deposition patterns on plasma facing components and can be an important contributor to fusion fuel retention due to the co-deposition. Two of the most important impurities are nitrogen (N), which is used as a seeding gas to promote radiative plasma cooling and, specifically, in the ASDEX Upgrade (AUG) tokamak, boron (B) which is used as a getter material to suppress the oxygen content on tungsten (W) plasma facing components in the tokamak vessel.

Ion beam analytical (IBA) methods with broad (≈1 mm^2) analysing beam are usually used to provide information on surface composition and concentration of impurities on samples exposed in tokamaks [1]. By means of a focused ion beam one can obtain additional information on the lateral distribution, on retained fuel and impurities on the micro-meter level mainly in the poloidal direction where variations are the greatest [2,3,4] assuming we have no leading edges or shadowed regions that can introduce large variations in toroidal direction.

Here we present the results of studies where focused ion beams have been applied to determine the distribution of plasma fuel (deuterium (D)) and two light impurities, boron (^{11}B) and nitrogen (^{15}N), on samples exposed in the divertor region of AUG machine during ^{15}N-seeded L-mode discharges in D [5] or during H-mode discharges in He [6,7]. This way, the effect of different operational conditions and plasma gases on the deposition profiles could be studied. The samples had different surface roughnesses, ranging from mirror like polished surface up to couple of μm features on the surface. Which had an contribution on the results. All the samples were mounted on a divertor manipulator arm which enables exposure of several small samples to divertor plasmas in the vicinity of the low-field side (outer) strike point [8].

2. Experimental set-up

For microbeam measurements we used the 2 MV tandem accelerator at Jožef Stefan Institute [9] coupled with a microbeam line, located at 10° from the exit port of the accelerator. The accelerator and the beam line are coupled with a high brightness multicusp ion source for producing a high brightness proton ion beam [10], which can be focused to dimensions down to 0.5x0.5 μm^2 at an energy of 3 MeV in a high current mode [11]. Light Z elements (Z<9) are generally detected by nuclear reaction analysis (NRA). To quantify the amount of D the D(^{3}He,p)α nuclear reaction was used [12,13]. We focused a 3.3 MeV ^{3}He ion beam down to

10x10 μm^2 in high current mode of 300 pA. For NRA measurements of ^{11}B and ^{15}N, which were quantified by the nuclear reactions $^{11}B(p,\alpha)^8Be$ [14,15] and $^{15}N(p,\alpha)^{12}C$ [16] , we used a focused proton beam at energies of 2.6 MeV and 1 MeV respectively. Both beams were focused down to 1.5x1.5 μm^2 in the high current mode. The dimensions of the ion beam are optimized with a knife edge method on a copper grid, using induced K_α X-ray emission and HP-Ge X-ray detector.

For the quantification of the measurement data, we used the cross sections available for these two nuclear reactions and compared the simulated signals to the experimental signal obtained from the calibrated boron and nitrogen standards. For B, an amorphous boron hydride (a-B:H, with B amount of $3x10^{18}$ B/cm^2 and H amount of $8x10^{17}$ H/cm^2) was used as standard while for ^{15}N, a sample with $3x10^{16}$ at/cm^2 of ^{15}N implanted into W was used.

The end station is equipped with a 5-axes manipulator and a microscope with a camera for sample positioning in the focal plane of the ion beam. In front of the end station a triplet of quadrupole magnetic lenses is used for focusing the ion beam and deflection coils for rastering the beam on the sample. With existing hardware, we are able to scan the beam across an area of 2200x2200 μm^2 and produce elemental maps with a resolution of 256x256 pixels. For dose normalization we use a beam chopper combined with an RBS detector [17].

A high-purity germanium X-ray detector is positioned at 135° with respect to the beam direction. It is used to reveal the concentrations and distribution of various metallic impurities on the samples by particle induced X-ray emission (PIXE) measurements. The detector is optimized for the detection of X-rays in the region from 3 to 54 keV. To study possible layered structure of the analyzed samples, a PIPS-type RBS detector with a 300 μm thick depletion layer is positioned at 135° with respect to the beam direction, covering a solid angle of 5.6 msr. It is equipped with an 0.8 μm thick Al foil serving as a light block filter. For spectroscopy of fast protons emitted from the nuclear reactions an NRA detector is positioned at 135° with respect to the primary beam direction. The NRA detector is a PIPS detector with a 1000 μm thick depletion layer and an active area of 300 mm^2. At mounted position the detector covers a solid angle of 0.14 sr. The detector is shielded by a thin Al foil which serves as visible light block. For measuring protons from the D reaction we used 6 μm of Al foil and 125 μm thick kapton foil while for the B and N reactions we used only 3 μm thick Al foil. This combination of foils also produces enough energy loss for the fast protons, to be completely stopped in the depleted layer of the NRA detector and is thick enough to stop backscattered ions (protons or ^3He) from the primary beam. The acquisition system is designed in a way that each detector event in the set of detectors is recorded and saved in a

list mode together with the information on the beam position. More details on the experimental set up are given in Ref. [4].

To obtain poloidal elemental profiles the measured 2D maps were projected along the line of interest. The obtained NRA and RBS spectra were analysed with the SIMNRA [18] program to calculate the concentrations and depth profiles of different elements. PIXE spectra were analysed using the GeoPIXE software [19] and errors of the obtained concentrations are estimated to be below 15%, which manly originate from inaccuracy of fitting and ion current measurements inaccuracy.

3. Results

We performed microbeam analyses on samples from the nitrogen-15 experiment. Samples were positioned on the divertor manipulator arm below (in the private flux region) and above the strike point. We analysed altogether 6 sample with three types of sample microstructure that were exposed on the manipulator arm on position number 2 and 3, as shown on Figure 1a. The first type of samples consists of 100 nm of W deposited on milled (samples labelled as M2, M3). The second type consists of 100 nm of W deposited polished fine grained graphite (samples labelled as P2, P3). The third type consists of bulk W samples (samples labelled as W2, W3). With such selection of samples we cowered large range of surface roughness where milled being roughest and bulk W being smoothest. The microbeam analysis consisted of 3 rectangular measurement spots across the poloidal direction at equidistant steps of 14.75 mm; along this line the changes in the plasma conditions during the exposure in AUG were the largest. The scanned areas are shown in Figure 1b for one of the samples from ^{15}N experiment .

In the ^{15}N experiment, all the samples were exposed to total of a 5.3×10^{21} ^{15}N atoms, which were injected during 5 L-mode discharges in D in AUG, details given in Ref. [5]. ^{15}N was used as the tracer since its natural abundance is only 0.4%, and thus contamination from surrounding air is negligible. The samples were exposed using the upgraded divertor manipulator arm of AUG [8] and according to Figure 1 were located poloidally on both sides of the outer strike point.

Two examples of a detailed 2D distribution map of the D amount obtained on samples M2 and P2 are shown in Figures 2a and 2b, respectively. The resolution of maps is determined by counting statics such that errors of the calculated values are below 10% and is lower than analytical beam resolution. The lateral distribution of the D amounts along the poloidal axis for all analysed AUG samples from the nitrogen-15 experiment is shown in Figure 2c. The D amount is on average $80\text{-}90 \times 10^{15}$ D/cm^2 for unpolished-milled graphite (M) samples, 30-

$40x10^{15}$ D/cm^2 for polished (P) graphite samples and $10\text{-}15x10^{15}$ D/cm^2 for W bulk sample. There is a clear trend of D retention dependence on surface roughness having more retention on the rough surface. There is also observed a small dependence of D retention on the analysing position, obtaining the largest retention near the strike point.

The detailed 2D distribution map of the ^{15}N amount is shown on Figures 3a and 3b, also for M2 and P2 samples. Whereas the lateral distribution of the ^{15}N amounts along the poloidal axis for all analysed samples is shown in Figure 3c. The average ^{15}N amounts are $5\text{-}13x10^{15}$ N/cm^2 as shown on a Figure 3 and are comparable to those obtained in Ref. [5]. As observed for the deuterium retention also in this case the largest ^{15}N content is obtained on W deposited on milled graphite samples. On bulk W samples the impurity retention is the lowest being $3\text{-}7x10^{15}$ N/cm^2. The 2D distribution maps for D and ^{15}N show no direct correlation of hot spots on a micrometer level. Due to the low counting statistics for boron we could not make the 2D distribution maps, therefore we show only the lateral distribution of B for all analysed samples in Figure 4. The B amount is between $20x10^{15}$ B/cm^2 and $30x10^{15}$ B/cm^2 for all three types of samples.

The variations of the retained D, N and B show some variation and vague correlation in poloidal direction inside of each scanning frame as shown in Figures 2c ,3c and 4. In both cases, the D and N amounts are larger on unpolished samples than on polished graphite samples. On bulk W samples the impurity retention is the lowest. The B distribution can be explained by B originating from residual B inventories on the vessel while D and N were directly injected during the discharges. We observed some W surface scratches in poloidal direction, probably due to arc traces on the surface of samples which cannot be correlated with impurity distributions. Other heavy impurities were measured by PIXE technique and found to be homogenously distributed over polished and unpolished graphite samples yielding around 900 μg/g of Ca, 400 μg/g of Ti, 450 μg/g of Cr and 4000 μg/g of Fe. In bulk W samples we detected only around 100 μg/g of Fe while Ca, Ti and Cr were below the detection limit.

From the helium experiment, 3 samples were selected for analyses, one of them being a bulk W sample (labelled as W2), second one a pre-damaged piece of bulk W (T3) where fuzz-like nanostructures were produced using a pure He 37 keV beam and He fluence of $1x10^{24}$ m^{-2} in the GLADIS facility [20], and the third sample was 20 nm of W coated on milled fine grain graphite (M2). Details on the He experimental campaign are given in Ref. [6,7]. The samples from the He experiment were only analysed with a 2.6 MeV proton beam, as the main focus was the analysis of B as impurity.

Analysed samples from the He experiment in AUG show inhomogeneous distribution of W with micro-scale roughness which is most pronounced on W coated sample (M2) and on pre-damaged sample (T3) where fuzz-like structure is visible on Figure 5. There we show the W PIXE maps and SEM images for the two samples, where nice correlation on microstructure can be observed by the two different imaging techniques. On the layered sample (20 nm of W on milled graphite) we observe a similar surface structure of W in a shape of snake skin as reported in [4].

In Figure 6a and 6b a detailed 2D distribution map of B is shown for M2 and T3 samples, respectively. The lateral distribution for all three samples on different analysing position along the poloidal axis is shown in Figure 6c. The retention of B is strongest in pre-damaged sample (T3) ranging between 2000-3500 $x10^{15}$ B/cm^2, while the B amount on W deposited on graphite (M2) and bulk W (W2) is 450-600 $x10^{15}$ B/cm^2 and around 100 $x10^{15}$ B/cm^2 respectively, as shown in Figure 6. The B amount on samples from the He experiment are substantially higher than in the case of ^{15}N campaign. Reason for this difference lies in the time sequence the way experiments were carried out. The He experiment was carried out shortly (days) after the boronization of the AUG vessel where on the other hand the ^{15}N experiment was performed long after the boronization. One more reason for the increased B amount in He experiment could be due to the He plasma discharge that could be more efficient in removing deposits from the main chamber and depositing them in the divertor region. For pre-damaged W sample we observe also large increase of heavy impurities like Ti, Cr and Fe yielding concentrations of 4000 μg/g, 300 μg/g, 950 μg/g, respectively, as compared to bulk W sample where Ti, Cr and Fe are almost on the detection limit (180 μg/g, 85 μg/g, 280 μg/g). Also high amounts of impurities were observed in M2 sample, 5500 μg/g of Ti, 1000 μg/g of Cr and 6500 μg/g of Fe. All the surface creatures (seen in W PIXE maps) and scratches on samples cannot be correlated to the B distribution.

Summary

In the presented study we have analysed W and W deposited samples exposed in the ASDEX Upgrade tokamak, during experiments where nitrogen-15 was injected into L-mode discharges in D and during non-seeded H-mode discharges in He. Focused ion beams with micro-meter lateral resolution were applied in these analyses. The main focus was on the use of nuclear reaction analysis for the detection of D, ^{11}B and ^{15}N. The analysis was executed in the microbeam experimental chamber coupled with 2 MV tandem accelerator.

For the samples exposed in the nitrogen-15 seeded plasma we observe a slight increase of retained D and ^{15}N in regions further from strike point and decrease of ^{11}B in the same

regions. This behavior is attributed to fact that the B is a residual impurity, being retained in the private flux region from boronization, while D and ^{15}N were actively introduced and migrated also around the strike point. On the micro-scale we observe small variation in impurity distribution inside of the scanned areas. We observed some difference of retained impurities between different types of samples. We found an increased retention in samples with W deposited on graphite base as compared to bulk W samples. Most of the differences in the impurity amount are associated with the sample roughness: bulk W being very smooth, polished sample then, and finally unpolished.

On pre-damaged W bulk sample from the He experiment we observed some W fuzz-like structures on the sample surface which cannot be correlated with other impurities distributions. On W coated on graphite sample we observe some W hot spot on the surface. Also bulk W samples show nonhomogeneous distribution of impurities on the surface.

Acknowledgments

This work has been carried out within the framework of the EUROfusion Consortium and has received funding from the Euratom research and training programme 2014-2018 under grant agreement No 633053. Work was performed under EUROfusion WP PFC. The views and opinions expressed herein do not necessarily reflect those of the European Commission.

References

[1] M. Mayer et al., J. Nucl. Mater. 363-365 (2007) 101-106
[2] H. Khodja et al., Nucl. Instr. Meth. B 266 (2008) 1425
[3] P. Petersson et al., Nucl. Instr. Meth. B 268 (2010) 1833
[4] M. Kelemen et al., Nucl. Instr. Meth. B 2017 in press, https://doi.org/10.1016/j.nimb.2017.01.072
[5] G. Meisl et al., Nucl. Mater. Energ. 2016 in press, https://doi.org/10.1016/j.nme.2016.10.023
[6] S. Brezinsek et al., Nucl. Mater. Energ. 2016 in press, https://doi.org/10.1016/j.nme.2016.11.002
[7] A. Hakola et al., Nucl. Fusion 57 (2017) 066015
[8] A. Herrmann et al., Fusion Eng. Des. 98-99 (2015) 1496
[9] P. Pelicon et al., Nucl. Instr. Meth. B 269 (2011) 2317
[10] P. Pelicon et al., Nucl. Instr. Meth. B 332 (2014) 229
[11] P. Vavpetič et al., Nucl. Instr. Meth. B 2017 in press, https://doi.org/10.1016/j.nimb.2017.01.023
[12] M. Mayer et al., Nucl. Instr. Meth. B 267 (2009) 506
[13] S. Markelj et al., J. Nucl. Mater. 469 (2016) 133
[14] M. Mayer et al., Nucl. Instr. Meth. B 143 (1998) 244-252
[15] M. Kokkoris et al., Nucl. Instr. Meth. B 268 (2010) 3539-3545
[16] F. B. Hagedorn et al., Phys. Rev. 108, 4 (1957) 1015
[17] K. Vogel-Mikus et al., Nucl. Instr. Meth. B 267 (2009) 2884

[18] M. Mayer, SIMNRA User's Guide: Report IPP 9/113, Max-Planck-Instutut für Plasmaphysik Garching, 1997.

[19] C. G. Ryan et al., Nucl. Instr. Meth. B 363 (2015) 42

[20] H. Greuner et al., Fusion Eng. Des. 75-79 (2005) 345-350

List of figure captions

Fig.1: a) Photograph of the samples mounted on the divertor manipulator arm in the ^{15}N experiment in AUG.

b) Photograph of one of the exposed samples with the regions analysed using microbeam techniques marked using black rectangles.

c) Photograph of the samples mounted on the divertor manipulator arm in the He experiment in AUG.

d) Photograph of two of the exposed samples with the regions analysed using microbeam techniques marked using white rectangles.

Fig.2: The D amounts for samples exposed in ASDEX Upgrade tokamak in nitrogen-15 seeding campaign: a) and b) 2D maps of D distribution with 366 μm resolution on M2 and P2 samples, respectively; c) The amounts of D plotted in poloidal direction for all analysed samples. The D amounts were measured with $D(^3He,p)\alpha$ nuclear reaction with focused 3.3 MeV ^3He beam and calculated from NRA yields with SIMNRA software [18].

Fig.3: The N amounts for samples exposed in ASDEX Upgrade tokamak in nitrogen-15 seeding campaign: a) and b) 2D maps of N distribution with 157 μm resolution on M2 and P2 samples, respectively; c) The N amounts plotted in poloidal direction for all analysed samples. The N amounts were measured with $^{15}N(p,\alpha)^{12}C$ nuclear reaction using a focused proton beam at energies of 1.0 MeV and calculated from NRA yields with SIMNRA software [18].

Fig.4: The B amounts for samples exposed in ASDEX Upgrade tokamak in nitrogen-15 seeding campaign plotted in poloidal direction for all analysed samples. The B amounts were measured with $^{11}B(p, \alpha)^8Be$ nuclear reaction using a focused proton beam at energies of 2.6 MeV and calculated from NRA yields with SIMNRA software [18].

Fig.5: Maps of W x-ray yield and secondary electron SEM images for 20 nm of W deposited on graphite (M2) and a pre-damaged W samples (T3) from ASDEX Upgrade He campaign a)

bulk W and b) pre-damaged W. The SEM images were done at Center electron microscopy and microanalysis (CEMM) of Jožef Stefan Institute.

Fig.6: The B amounts for samples exposed in ASDEX Upgrade tokamak in He campaign: a) and b) show 2D maps of B distribution with 157 μm or 75 μm (finer maps) resolution on M2 and T3 samples, respectively; c) the amount of B plotted in poloidal direction for all analysed samples is shown. The B amounts were measured with $^{11}B(p,\alpha)^{8}Be$ nuclear reaction using a focused proton beam at energies of 2.6 MeV and calculated from NRA yields with SIMNRA software [18].

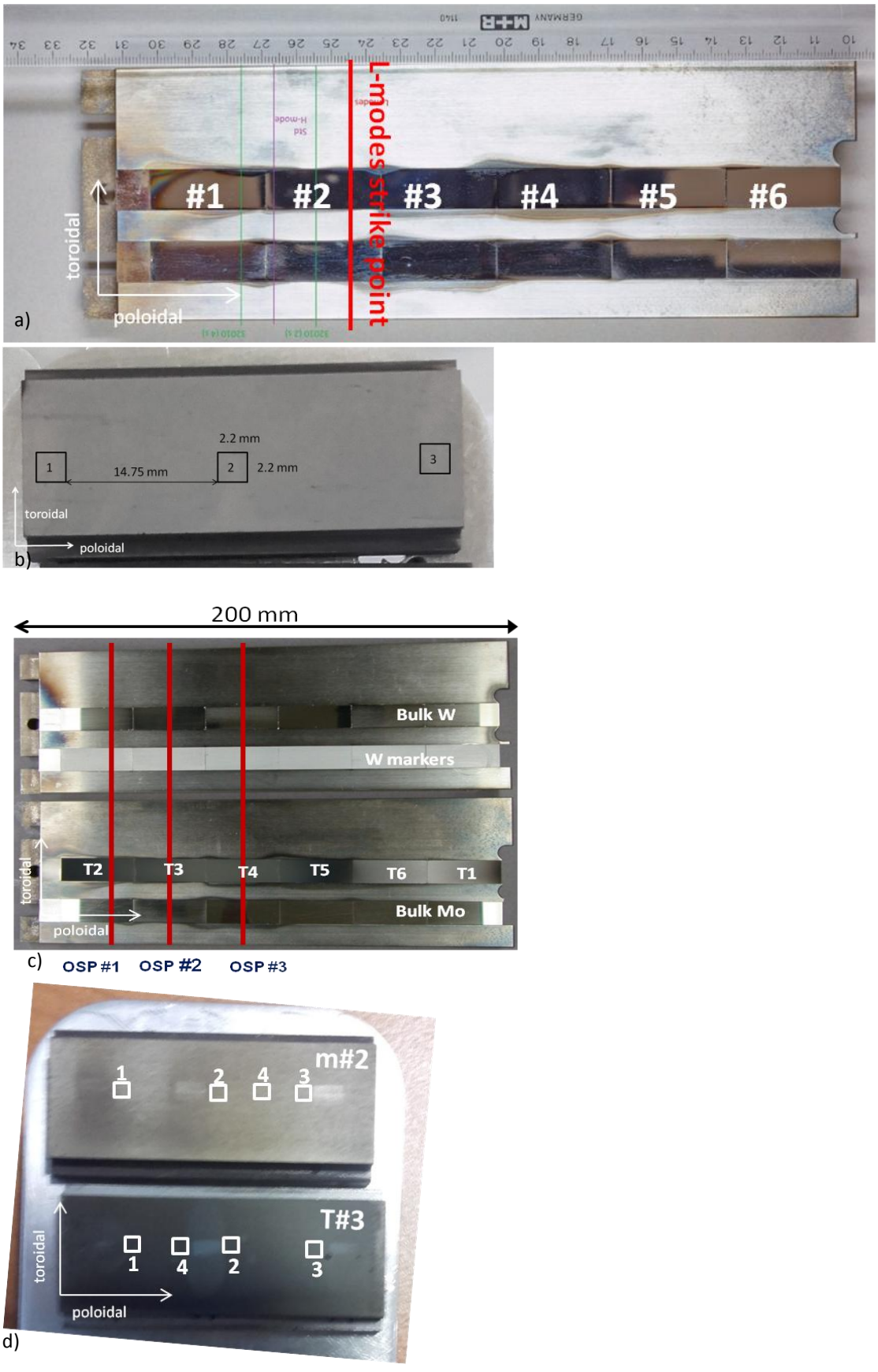
#1
#2
#3
#4
#5
#6
L-modes strike point
toroidal
poloidal
a)
2.2 mm
1
14.75 mm
2
2.2 mm
3
toroidal
poloidal
b)
200 mm
Bulk W
W markers
T2
T3
T4
T5
T6
T1
Bulk Mo
toroidal
poloidal
c)
OSP #1
OSP #2
OSP #3
m#2
1
2
4
3
T#3
1
4
2
3
toroidal
poloidal
d)

Figure 1

312

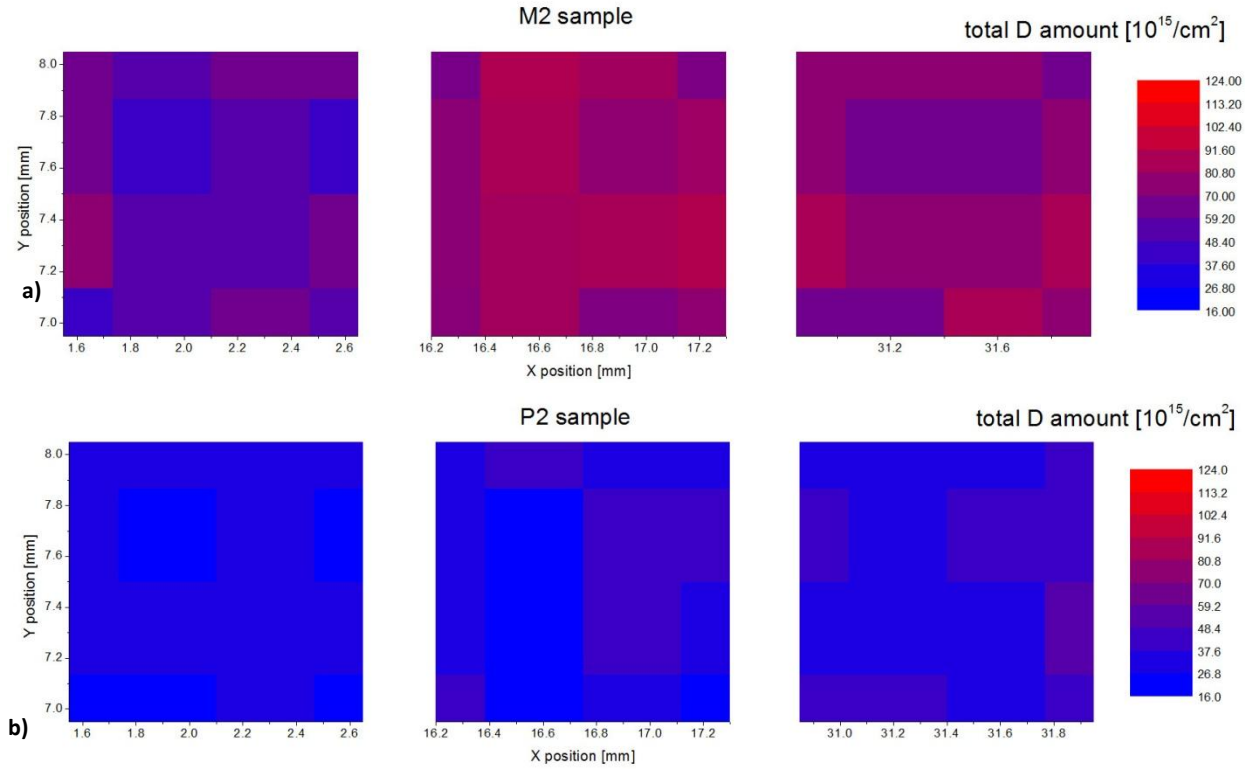

313

314

315

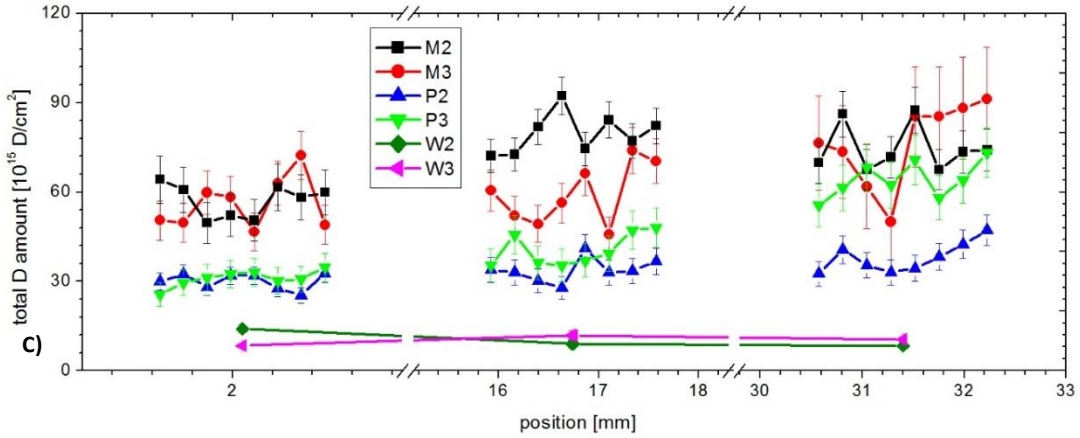

316

Figure 2

317

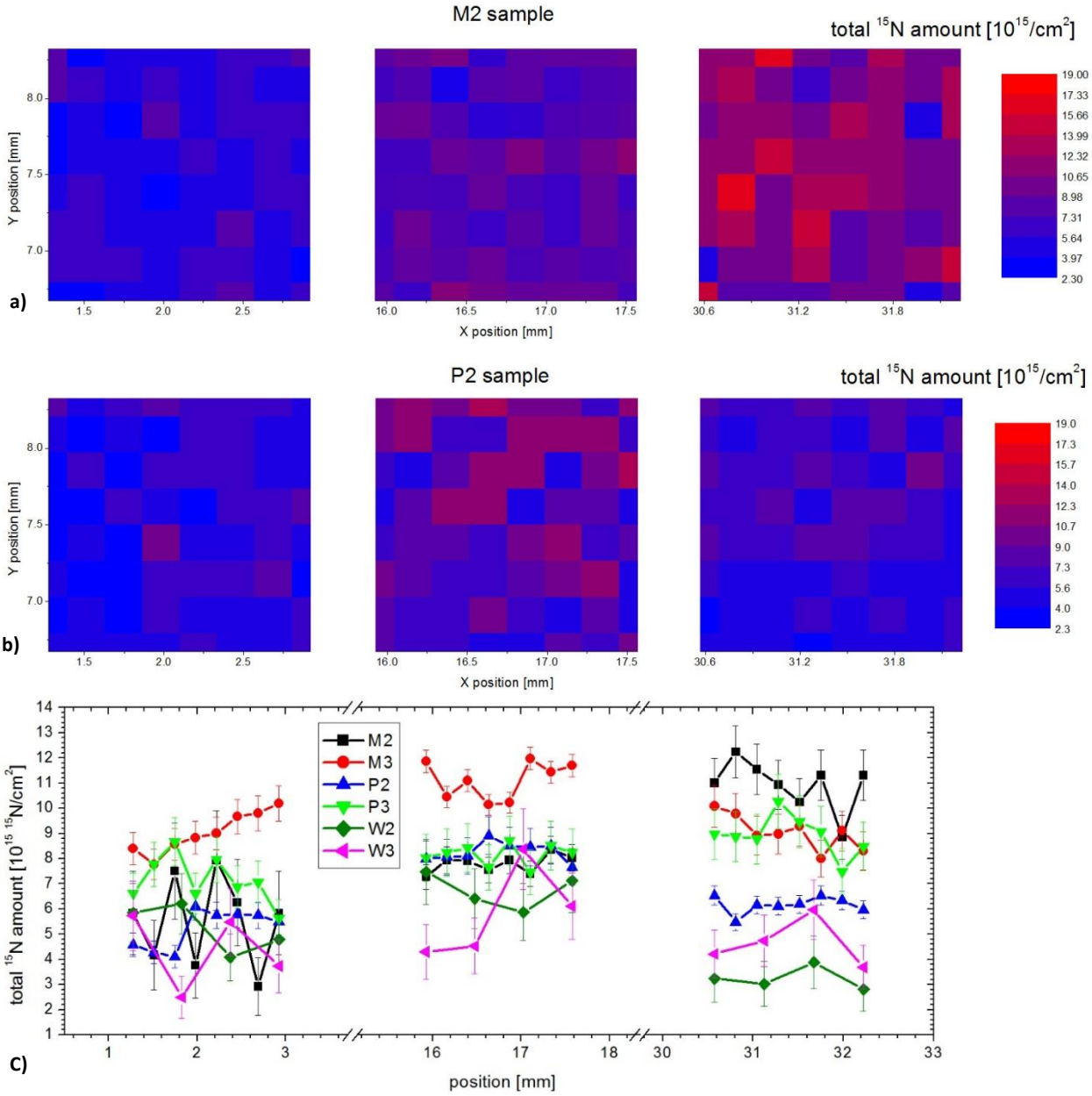
M2 sample
total ^{15}N amount [10^{15}/cm^2]
Y position [mm]
X position [mm]
a)
P2 sample
b)
M2
M3
P2
P3
W2
W3
total ^{15}N amount [10^{15} ^{15}N/cm^2]
position [mm]
c)

Figure 3

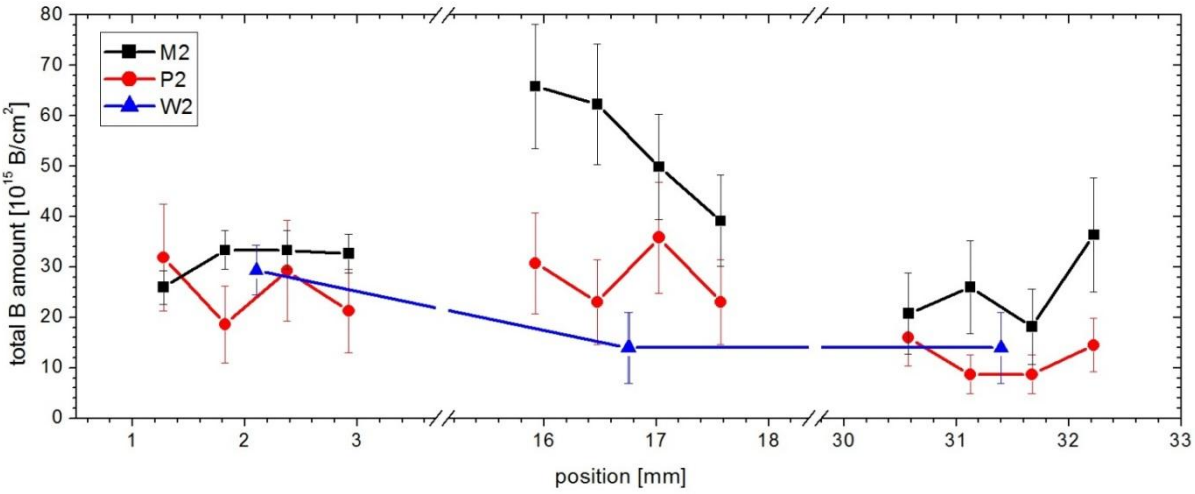
M2
P2
W2
total B amount [10^15 B/cm^2]
position [mm]
0
10
20
30
40
50
60
70
80
1
2
3
16
17
18
30
31
32
33

Figure 4

322

323

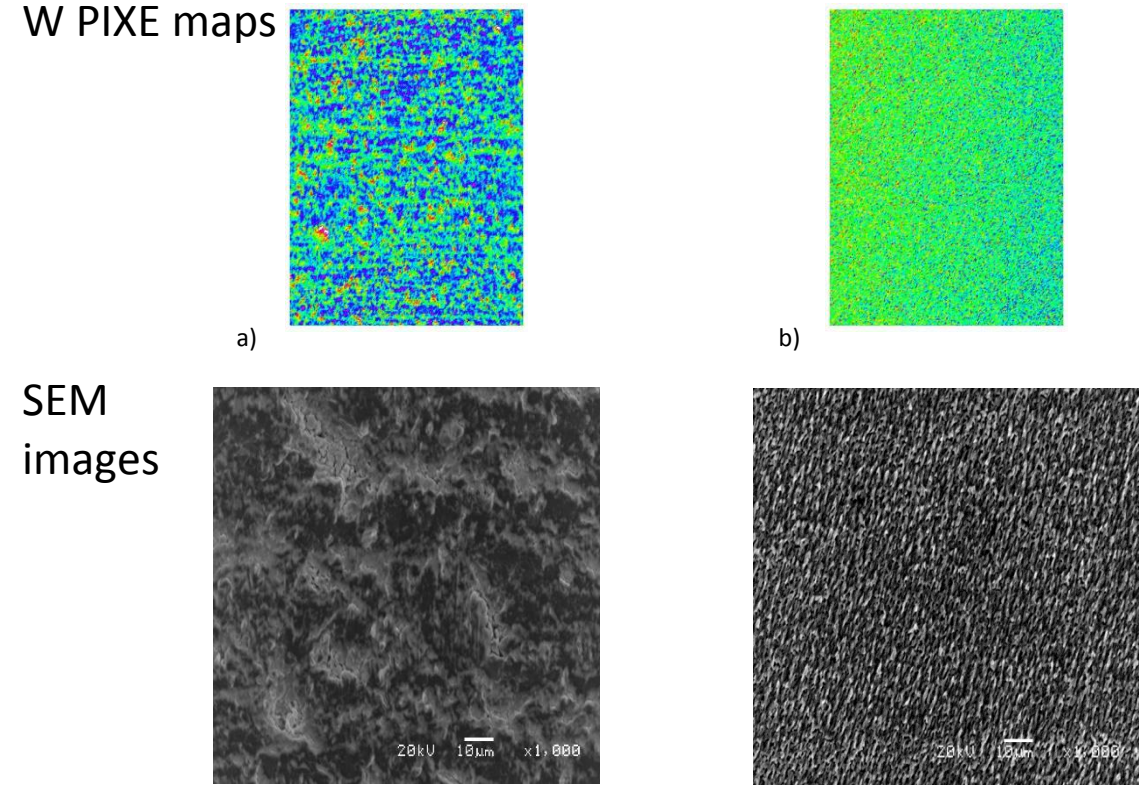

Figure 5

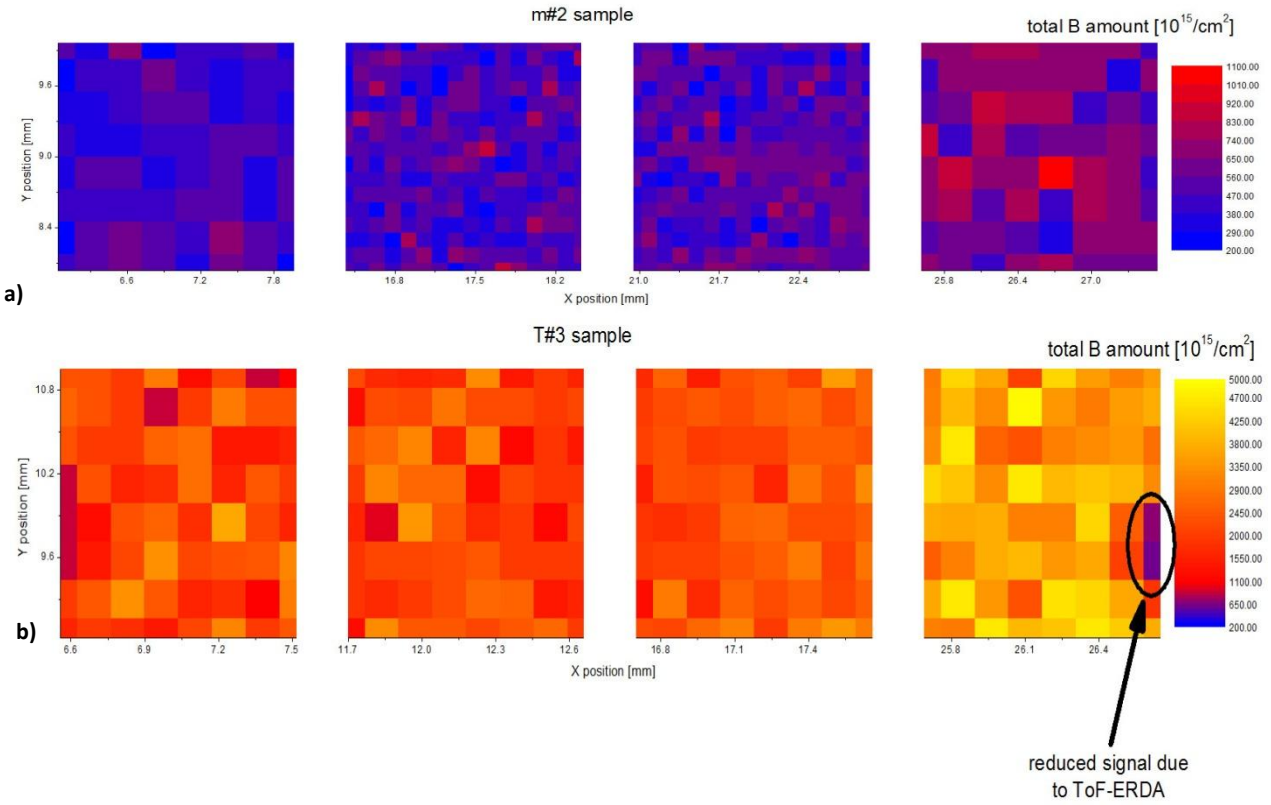
m#2 sample
total B amount [10^15/cm^2]
Y position [mm]
X position [mm]
a)
T#3 sample
total B amount [10^15/cm^2]
Y position [mm]
X position [mm]
b)
reduced signal due
to ToF-ERDA

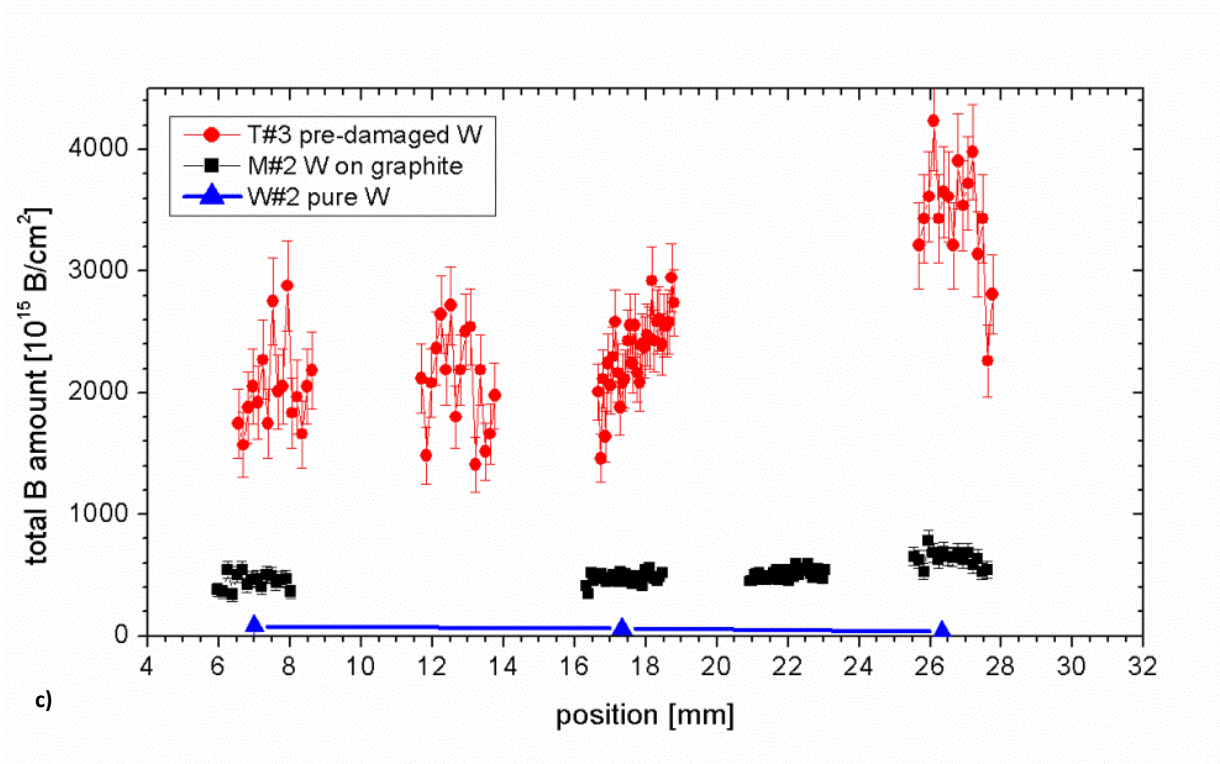
T#3 pre-damaged W
M#2 W on graphite
W#2 pure W
total B amount [10^15 B/cm^2]
position [mm]
c)

Figure 6